Composite solitary waves in three-component scalar field theory: II. Three-body low-energy scattering

A. Alonso Izquierdo[a] and J. Mateos Guilarte[b]

[a] *Departamento de Matematica Aplicada, Universidad de Salamanca, SPAIN*
[b] *Departamento de Fisica Fundamental and IUFFyM, Universidad de Salamanca, SPAIN*

Abstract

We discuss time evolution of some solitary waves described in the first part of this work. The adiabatic motion of the non-linear non-dispersive waves composed of three lumps is interpreted as three-body low energy scattering of these particle-like kinks.

1 Introduction

After a brief summary of the stability properties of the solitary waves discovered in the first part we shall devote this second part to the analysis of low energy dynamics. Study of Manton's adiabatic motion of solitary waves [22] is very simple in this case because the geometric metric of the moduli (parameter) space that governs the dynamics does not depend on the translational parameter x_0; thus, it is always possible to apply a transformation that leads to an Euclidean metric. On the other hand, there are only a few works that have addressed research into solitary waves in three-component scalar field theory models, see [23, 24, 25, 26]. In this richer case there are three-parametric families of kinks, and the adiabatic evolution of three-body lumps is associated with metrics with curvature. The low-energy dynamics of, in this case, three-body solitary waves is therefore much more intricate.

In this paper, we shall address a three-component scalar field model that generalizes the two-component model discussed in Reference [14] to three fields. The organization of the paper is as follows: In Section 1 some remarks about the stability of these solutions are given. Finally, in Section 2 we shall describe the adiabatic evolution on the moduli space of solutions of configurations composed of three basic lumps.

2 Some remarks about the stability of solitary waves

In order to analyze the stability of the solitary wave solutions, we shall apply different procedures. The direct approach is study of the spectrum of the second-order fluctuation (Hessian) operator –formula (10) in part I–, now around kink solutions. A non-negative spectrum of the kink Hessian operator ensures that a particular solitary wave solution is stable. Zero eigenvalues in the spectrum, zero modes, show that certain perturbations send static solutions into static solutions. Thus, zero modes are associated to neutral equilibrium directions in a sub-space of the configuration space where the adiabatic evolution of solitary waves takes place. It is easy to check that the existence of a kink family $\bar{\phi}(x, c)$ bears the presence of an eigenfunction $\frac{\partial \bar{\phi}}{\partial c}$ that belongs to the kernel of $\mathcal{H}$, i.e., $\frac{\partial \bar{\phi}}{\partial c}$ is a zero mode. When detailed information about the spectrum of the Hessian is lacking, an interesting procedure to study the stability of kink families is the application of Morse index theorem. A point –referred to as a conjugate or focal point– that is crossed by all the members of this family implies the existence of a negative eigenvalues in the spectrum of the Hessian operator [34, 35].

2.1 Stability of basic solitary waves

Let us consider first basic solitary waves, i.e., the K_1^{OB}, K_1^{CD} and K_1^{BC} kinks.

1. K_1^{OB} kink. Because only the third component is non-null, the Hessian is a diagonal 3×3-matrix differential operator with entries:

$$\mathcal{H}_{11} = -\frac{d^2}{dx^2} + 1 + \bar\sigma_3^4 + (1 - \sigma_3^4) \tanh \sqrt{2}\bar\sigma_3^2 \bar x - \frac{3}{2}\bar\sigma_3^4 \mathrm{sech}^2 \sqrt{2}\bar\sigma_3^2 \bar x$$

$$\mathcal{H}_{22} = -\frac{d^2}{dx^2} + 1 - 2\sigma_2^2\bar\sigma_2^2 - \sigma_3^2(2\sigma_2^2 - \sigma_3^2) + \bar\sigma_3^2(1 + \sigma_3^2 - 2\sigma_2^2)\tanh \sqrt{2}\bar\sigma_3^2 \bar x - \frac{3}{2}\bar\sigma_3^4 \mathrm{sech}^2 \sqrt{2}\bar\sigma_3^2 \bar x$$

$$\mathcal{H}_{33} = -\frac{d^2}{dx^2} + \frac{1}{2}\bar\sigma_3^4(10 + 6\tanh \sqrt{2}\bar\sigma_3^2 \bar x - 15\,\mathrm{sech}^2 \sqrt{2}\bar\sigma_3^2 \bar x) \qquad .$$

The spectral problem is fully solvable because we are dealing with three ordinary Schrödinger operators of the Posch-Teller type. $\mathcal{H}_{11}$ and $\mathcal{H}_{22}$ govern orthogonal fluctuations to the kink orbit in internal space, whereas $\mathcal{H}_{33}$ takes into account fluctuations tangent to the orbit. There are no discrete eigenvalues in the spectrum of $\mathcal{H}_{11}$ and $\mathcal{H}_{22}$, all the eigenfunctions belonging to the continuous spectrum. In the first case, the continuous spectrum starts at the threshold $\frac{\sigma_3^2}{\bar\sigma_3^4}$; $\omega^2(q) = q^2 + \frac{\sigma_3^2}{\bar\sigma_3^4}$ is a non-degenerate eigenvalue in the $[\frac{\sigma_3^2}{\bar\sigma_3^4}, \frac{1}{\bar\sigma_3^4}]$ interval but it is doubly degenerate for higher values of ω^2. In the second case, the threshold is $\frac{\sigma_{32}^4}{\bar\sigma_3^4}$ and the doubly degenerate spectrum starts at $\frac{\bar\sigma_2^4}{\bar\sigma_3^4}$. On the other hand, $\frac{\partial\phi}{\partial x}$ is a discrete eigenfunction of $\mathcal{H}_{33}$ with $\omega^2 = 0$ eigenvalue (zero mode) due to spontaneous breaking of translation symmetry by the kink solution. The continuous spectrum $\omega^2 = q^2 + 2\bar\sigma_3^4$ is non-degenerate for $\omega^2 \in [2\bar\sigma_3^4, 8\bar\sigma_3^4]$ and doubly degenerate for $\omega^2 \geq 8\bar\sigma_3^4$. In conclusion, the lack of non-negative eigenvalues allows us to claim the stability of this solution.

The Hessian for any other solitary wave solution is a non-diagonal matrix operator and the task of solving the spectral problem becomes hopeless. There is, however, a loophole to avoid this problem (not of necessary use in the K_1^{OB} case). On the ϕ_3 axis, the Hamilton characteristic function –formula (25) in part I– becomes:

$$W(\phi_3) = \frac{1}{\sqrt{8}}\left[(\phi_3^2(x) - 1)^2 + 2\sigma_3^2\phi_3^2(x)\right] \qquad .$$

The K_1^{OB}-kink orbit is a flow line of the gradient of W, a polynomial function. Thus, the energy is given by $|W(\bar\phi^O) - W(\bar\phi^B)|$, a topological bound, the absolute minimum of E in the $\mathcal{C}^{OB}$ topological sector. Therefore, K_1^{OB} is stable.

2. K_1^{CD} kink. In this case the Hessian is not diagonal but the alternative argument works exactly in the same manner. –formula (25) in part I– now reduces to:

$$W(\phi_1, \phi_2) = \frac{1}{\sqrt{8}}\left[(\phi_1(x) + \phi_2^2(x) - 1)^2 + 2\sigma_2^2\phi_2^2(x)\right] \qquad .$$

Again, $|W(\bar\phi^C) - W(\bar\phi^D)|$ is the absolute minimum of E in the $\mathcal{C}^{CD}$ topological sector and the K_1^{OB} kink is stable.

3. K_1^{BC} kink. The same argument also works with

$$W(\phi_2, \phi_3) = \frac{1}{\sqrt{8}}\left[(\phi_2(x) + \phi_3^2(x) - 1)^2 + 2\sigma_2^2\phi_2^2(x) + 2\sigma_3^2\phi_3^2\right]$$

and $E(K_1^{BC}) = |W(\bar\phi^B) - W(\bar\phi^C)|$, guaranteeing the stability of K_1^{BC}.

2.2 Stability of two-body solitary waves

The general Hessian operator for $K_2^{OC}(b)$ and $K_2^{BD}(b)$ kinks is a non-diagonal 3×3 matrix differential operator with an unknown spectrum. It is possible, however, to apply the Morse index theorem, see [34, 35]. Note in Figures 5(c) and 6(c) that there are no conjugate points -points where all the trajectories meet- in the congruence of kink trajectories of this type; the Morse index theorem relating the number of conjugate points to the number of negative eigenvalues of the Hessian reveals that both the $K_2^{OC}(b)$ and $K_2^{BD}(b)$ families are formed by stable kinks. The absence of conjugate points is due to the fact that the reduced Hamilton characteristic functions –formula (25) in part I– for both kinds of solitary waves are regular functions with no conical singularities where the gradient flow of W would be undefined.

This result is confirmed directly for a particular member, $K_2^{OC}(0)$, of the first family. In this case the Hessian operator –formula (10) in part I– is diagonal, with the following entries:

$$
\mathcal{H}_{11} = -\frac{d^2}{dx^2} + 1 + \sigma_2^4 + (1 - \sigma_2^4)\tanh\sqrt{2}\bar{\sigma}_2^2 x - \frac{3}{2}\bar{\sigma}_2^4 \operatorname{sech}^2\sqrt{2}\bar{\sigma}_2^2 x
$$

$$
\mathcal{H}_{22} = -\frac{d^2}{dx^2} + \frac{1}{2}\bar{\sigma}_2^4(10 + 6\tanh\sqrt{2}\bar{\sigma}_2^2 x - 15\operatorname{sech}^2\sqrt{2}\bar{\sigma}_2^2 x)
$$

$$
\mathcal{H}_{33} = -\frac{d^2}{dx^2} + 1 - 2\sigma_3^2\bar{\sigma}_3^2 - \sigma_2^2(2\sigma_3^2 - \sigma_2^2) + \bar{\sigma}_2^2(1 + \sigma_2^2 - 2\sigma_3^2)\tanh\sqrt{2}\bar{\sigma}_2^2\bar{x} - \frac{3}{2}\bar{\sigma}_2^4\operatorname{sech}^2\sqrt{2}\bar{\sigma}_2^2\bar{x}
$$

and the analysis of the spectral problem is as follows: there are no discrete eigenvalues in the spectrum of $\mathcal{H}_{11}$. The continuous spectrum $\omega^2(q) = q^2 + \frac{\sigma_2^2}{\bar{\sigma}_2^4}$ starts at the threshold $\frac{\sigma_2^2}{\bar{\sigma}_2^4}$ and is non-degenerate in the $[\frac{\sigma_2^2}{\bar{\sigma}_2^4}, \frac{1}{\bar{\sigma}_2^4}]$ interval but doubly degenerate for higher values. $\frac{\partial\bar{\phi}}{\partial x}$ is a zero mode of $\mathcal{H}_{22}$ due to spontaneous symmetry breaking of translational invariance by the solitary wave. The continuous spectrum $\omega^2 = q^2 + 2\bar{\sigma}_2^4$ is non-degenerate for $\omega^2 \in [2\bar{\sigma}_2^4, 8\bar{\sigma}_2^4]$ and doubly degenerate for $\omega^2 \geq 8\bar{\sigma}_2^4$. Finally, the third component, $\mathcal{H}_{33}$, has a zero mode with eigenfunction $\frac{\partial\bar{\phi}}{\partial a}(0)$ due to motion without energy cost in the space of kink orbits. We find a continuous spectrum, which is non degenerate in the range $[\frac{\sigma_{32}^4}{\bar{\sigma}_2^4}, \frac{\bar{\sigma}_3^4}{\bar{\sigma}_2^4}]$ and doubly degenerate from this value. Again all the eigenvalues are non-negative and the stability of this solution is established.

2.3 Stability of three-body solitary waves

The $K_3^{OD}(a, b)$ kinks, encompassing the three basic kinks with no static forces between them, form a set of distinguished solitary waves of this system. One- and two-body solitary waves arise in this model because of the embedding of lower dimensional systems of the same type. They are generic in the sense that this variety of solutions depends on as many parameters -two apart from the center of the kinks- as possible for a three-component scalar field theory. Moreover, the stability of this two-parametric kink family is easily established by a quick and visual application of the Morse index theorem. Away from the vacuum points, $\bar{\phi}^O$ and $\bar{\phi}^D$, the $K_3^{OD}(a, b)$ kink orbits do not intersect; there are no conjugate points, see Figure 7(c). Being the gradient flow lines of W –formula (25) in part I–, conjugate points cannot exist because W is a regular function and the flow is well defined. Therefore, these solutions are stable.

Although the Hessian operator is a very complicated 3×3 non-diagonal matrix differential operator and although the spectrum is essentially unknown, it is easy to prove the existence of three zero modes: 1) $\frac{\partial\bar{\phi}_a}{\partial x}(x; a, b)$, 2) $\frac{\partial\bar{\phi}_a}{\partial a}(x; a, b)$, and 3) $\frac{\partial\bar{\phi}_a}{\partial b}(x; a, b)$. Given a one-parametric family of solutions $\bar{\phi}_a(x; \alpha)$, simply differentiate both sides of the static field equations with respect to the parameter:

$$
\frac{d^2\bar{\phi}_a}{dx^2}(x; \alpha) = \frac{\partial V}{\partial\phi_a}\Big|_{\vec{\phi}}(x; \alpha) \qquad \Rightarrow \qquad \frac{d^2}{dx^2}\cdot\frac{\partial\bar{\phi}_a}{\partial\alpha}(x; \alpha) = \sum_{b=1}^{3}\frac{\partial^2 V}{\partial\phi_a\partial\phi_b}\Big|_{\vec{\phi}}(x; \alpha)\cdot\frac{\partial\bar{\phi}_a}{\partial\alpha}(x; \alpha) \qquad .
$$

On the other hand, the spectral problem is solvable for a particular member, the $K_3^{OD}(0,0)$ kink, living in the ϕ_1 axis. The operator is diagonal with entries

$$\mathcal{H}_{11} = -\frac{d^2}{dy^2} + 5 - 3\tanh\sqrt{2}y - \frac{15}{2}\operatorname{sech}^2\sqrt{2}y$$

$$\mathcal{H}_{22} = -\frac{d^2}{dy^2} + 1 - 2\sigma_2^2 + 2\sigma_2^4 + (1 - 2\sigma_2^2)\tanh\sqrt{2}y - \frac{3}{2}\operatorname{sech}^2\sqrt{2}y$$

$$\mathcal{H}_{33} = -\frac{d^2}{dy^2} + 1 - 2\sigma_3^2 + 2\sigma_3^4 + (1 - 2\sigma_3^2)\tanh\sqrt{2}y - \frac{3}{2}\operatorname{sech}^2\sqrt{2}y$$

where $y = x + \frac{1}{\sqrt{2}}\log\frac{\sigma_2\sigma_3}{\bar{\sigma}_2\bar{\sigma}_3}$. $\mathcal{H}_{11}$ governs the behavior of the fluctuations tangent to the orbit on the solution whereas $\mathcal{H}_{22}$ and $\mathcal{H}_{33}$ govern the orthogonal perturbations to the kink orbit, pushing the solution towards another with non-null values of a and b. The discrete spectrum of $\mathcal{H}_{11}$ comprises only a zero mode whose eigenfunction is $\frac{\partial\bar{\phi}}{\partial x}$, whereas the continuous spectrum $\omega^2 = q^2 + 1$ is non-degenerate for $\omega^2 \in [1,4]$ and doubly degenerate for values greater than 4. Likewise $\mathcal{H}_{22}$ presents a zero mode with eigenfunction $\frac{\partial\bar{\phi}}{\partial a}$ and the continuous spectrum is non degenerate in the range $[2\sigma_2^4, 2\bar{\sigma}_2^4]$; doubly degeneracy of the spectrum starts from this value. Finally, $\mathcal{H}_{33}$ holds a zero mode with eigenfunction $\frac{\partial\phi}{\partial b}$ and $[2\sigma_3^4, 2\bar{\sigma}_3^4]$ and $(2\max\{\sigma_3^4, \bar{\sigma}_3^4\}, \infty)$ are respectively the ranges of the singly and doubly degenerate continuous spectrum. We conclude the stability of this solution.

2.4 Instability of four-body, six-body and seven-body solitary waves

Note that the $K_4^{BB}(b)$ and $K_4^{CC}(b)$ kink trajectories always meet at a common point: the conjugate point, see Figure 11(c) and 12(c). For the K_4^{BB} family, this point is the focus F_1, whereas for the family K_4^{CC} it is one of umbilicus points A of $\mathbb{E}$. This is the signal of the instability of these solutions: according to the Morse index theorem, the Hessian for any member of these families has a negative eigenvalue [34, 35]. The undefined flow at the foci of the ellipse e_1 or the umbilical points of the ellipsoid $\mathbb{E}$ arise because the sign combinations in the Hamilton characteristic function providing these trajectories are such that, back in Cartesian coordinates, W is a function which is non-differentiable at either F_1 or A. Thus, these are flow lines obtained by gluing two flow lines generated by different Hamilton characteristic functions at these points. The energy depends not only on the value of the Hamilton function at the beginning and the end of the orbit but also on the values at the conjugate points. The absolute minimum value of the energy in the corresponding topological sector is non-saturated and four-body kinks are unstable.

For the one-parametric six-body $K_6^{CC}(b)$ and $K_6^{BB}(b)$ kink families, the situation is exactly the same. There exists a conjugate point, which is crossed by all the members of each family. For the $K_6^{CC}(b)$ it is the focus F_2 of the ellipse e_2, and for the $K_6^{BB}(b)$ it is the focus F_3 of the ellipse e_3. Again, application of the Morse index theorem and considerations on the impossibility of reaching the absolute minimum of the energy when there are conjugate points reveal the instability of six-body lumps.

The case of seven-body solitary waves $K_7^{BC}(\gamma_2, \gamma_3)$ is more complicated. There exist focal lines, curves of conjugate points; on each point of the characteristic hyperbola h a whole one-parametric subfamily of trajectories meet. The same is true for a point in the characteristic ellipse e_4. The Morse index theorem tells us that the Hessian for these solutions has two negative eigenvalues. Furthermore, the absolute minimum of the energy is not reached by $K_7^{BC}(\gamma_2, \gamma_3)$ kinks because of the existence of lines of conjugate points crossed by the kink orbits: the instability of seven-body solitary waves is proved.

The dynamical reason for the instability of these solitary waves is the peculiar configuration of the lumps arranged in these solutions. All these solitary waves are static solutions formed by several basic particles, where some of these lumps travel superposed. Because they are static solutions, the lumps are distributed in order to achieve an equilibrium configuration where no forces between lumps are involved: the exact overlapping between lumps produces this balance of forces. Any small perturbation slightly

4

splitting the superposed lumps breaks the unstable equilibrium releasing forces between the lumps. The negative eigenvalues of the Hessian operator associated with this process indicate that the evolution of these solitary waves moves them away from the initial static configurations.

3   Three-body low-energy scattering of non-linear waves

The three parameters x_0, a and b of the K_3^{OD} family of solitary waves fix the center of mass and the relative positions of the basic lumps in the composite kink configuration. We shall now study the evolution of composite solitary waves within the framework of Manton's adiabatic principle, see [21, 22], by looking at changes in a and b in time. The Manton adiabatic hypothesis can be summarized as follows: the dependence on time of solitary waves develops only in the parameters of the solution, i.e. $\bar{\phi}^K(x;t) = \bar{\phi}^K(x; a(t), b(t))$. This is a good approximation if the kink evolution is so slow that the differential equations –formula (5) in part I– are satisfied at every given t with good accuracy.

The most general family of trajectories arising in a N-dimensional Hamiltonian system depends on $2N$ parameters: N separation constants and N integration constants. Finite action fixes the separation constants at a fixed value. Therefore, the most general family of solitary waves in N-component scalar field theory depends on N parameters, the integration constants of the finite action trajectories in the analogous mechanical system. In this case adiabatic evolution is of the general form:

$$\bar{\phi}_a^K(x;t) = \bar{\phi}^K(x; a^I(t)) \quad , \quad a = 1, 2, \cdots, N \quad , \quad I = 1, 2, \cdots, N$$

Introducing this assumption in the action functional, (**??**) one obtains the action for a geodesic problem:

$$S^G = \frac{1}{2} \int dx\, dt \sum_{a=1}^{N} \frac{\partial \bar{\phi}_a^K}{\partial t} \frac{\partial \bar{\phi}_a^K}{\partial t} = \frac{1}{2} \int dt \sum_{I,J=1}^{N} g_{IJ}(a^K) \frac{da^I}{dt} \frac{da^J}{dt} \quad ,$$

where the metric tensor $g_{IJ}(a^K)$, the Christoffel symbols Γ_{IJ}^K, and the curvature tensor are:

$$g_{IJ}(a^K) = \sum_{a=1}^{N} \int_{-\infty}^{\infty} dx\, \frac{\partial \bar{\phi}_a^K}{\partial a^I} \frac{\partial \bar{\phi}_a^K}{\partial a^J} \quad , \quad \sum_{K=1}^{N} g_{MK} \Gamma_{IJ}^K = \sum_{i=1}^{N} \int_{-\infty}^{\infty} dx\, \frac{\partial \bar{\phi}_i}{\partial a^M} \frac{\partial^2 \bar{\phi}_i}{\partial a^I \partial a^J}$$

$$R_{IJKM} = \sum_{i=1}^{n} \int_{-\infty}^{\infty} dx \left[\frac{\partial^2 \bar{\phi}_i^K}{\partial a^I \partial a^K} \frac{\partial^2 \bar{\phi}_i^K}{\partial a^M \partial a^J} - \frac{\partial^2 \bar{\phi}_i^K}{\partial a^I \partial a^M} \frac{\partial^2 \bar{\phi}_i^K}{\partial a^K \partial a^J} \right] \quad , \quad R_{IJKM} + R_{IKMJ} + R_{IMJK} = 0 \quad ,$$

$$R_{IJKM} = -R_{JIKM} = -R_{IJMK} = R_{JIMK} = R_{KMIJ} \quad .$$

Study of the evolution of solitary waves thus turns into a geometric problem in the adiabatic regime: the analysis of geodesic motion in the moduli space of parameters where a non-Euclidean metric is inherited from the dynamics of the zero modes. The geodesics obey the associated Lagrange equations:

$$\frac{d^2 a^K}{dt^2} + \sum_{I,J=1}^{n} \Gamma_{IJ}^K \frac{da^I}{dt} \frac{da^J}{dt} = 0 \ ; \ K = 1, \ldots, N \tag{1}$$

Back in our $N = 3$ scalar field theory we consider $a^{I=1} = a$ and $a^{I=2} = b$ as local coordinates in the moduli space of parameters for $K_3^{OD}(a, b)$ three-body solitary waves. Both the dynamics and the geometry of the center of mass determined by the x_0 parameter are trivial: the component $g_{x_0 x_0}$ is constant, the geodesics being straight lines $x_0 = \mathrm{v}\, t + d$. Therefore, the dynamics of the center of mass obeys Galilean, rather than Lorentzian, velocity transformations in the adiabatic regime. Choosing the

values of the coupling constants $\sigma_3^2 = 2\sigma_2^2 = \frac{1}{3}$ and defining the variable $z = e^{\frac{2\sqrt{2}x}{3}}$ as in Section §3, we obtain the following integral expressions for the components of the metric tensor:

$$g_{aa}(a,b) = \int_0^\infty \frac{2(1 + b^2 z^2 + z^3)^2 + a^2(3z + b^2 z^3)}{2\sqrt{2}(1 + a^2 z + b^2 z^2 + z^3)^3} dz \tag{2}$$

$$g_{ab}(a,b) = \int_0^\infty \frac{-abz^3(a^2 + 2b^2 z + 3z^2)}{2\sqrt{2}(1 + a^2 z + b^2 z^2 + z^3)^3} dz \tag{3}$$

$$g_{bb}(a,b) = \int_0^\infty \frac{z[(a^4 + 3b^2)z^2 + (1 + z^3)^2 + 2a^2 z(1 + b^2 z^2 + z^3)]}{2\sqrt{2}(1 + a^2 z + b^2 z^2 + z^3)^3} dz \quad . \tag{4}$$

Integrals of rational functions in (2), (3) and (4) would be feasible but, depending on the arbitrary parameters a and b, the quadratures involved in this calculation lead to expressions that are so complicated that there is no advantage in addressing the problem analytically. Numerical integration, however, gives us interesting qualitative information about the metric tensor and the scalar curvature. In Figure 16, the components of the metric tensor as well as the scalar curvature are displayed as a function of a and b.
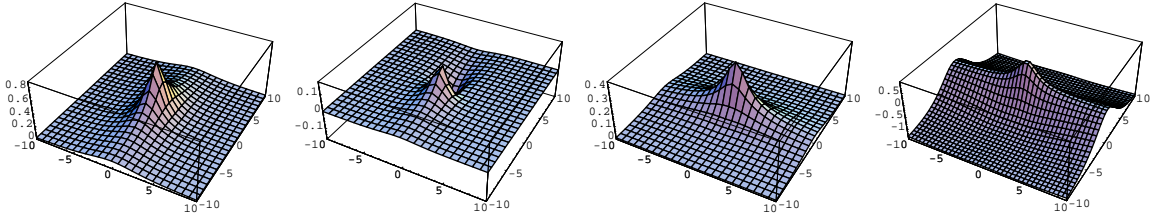

Figure 16: *Metric Components and Scalar Curvature: a) $g_{aa}(a,b)$, b) $g_{ab}(a,b)$, c) $g_{bb}(a,b)$, d) $R(a,b)$.*

The picture of the scalar curvature is especially useful for obtaining clues about geodesic motion. In regions where the curvature is positive the geodesics tend to approach each other whereas where it is negative the geodesics move away. Therefore, a certain interaction between lumps arises in the study of the evolution of solitary waves even in the adiabatic approximation. Recall that $K_3^{OD}(x; a, b)$ solitary waves are stable and the zero modes are the lowest energy eigenfunctions of the Hessian operator; low-energy fluctuations are dominated mainly by these channels, certifying the efficacy of the adiabatic procedure. For this reason, the adiabatic method is not applicable to unstable configurations, such as four-body, $K_4^{BB}(b)$ or $K_4^{CC}(b)$, six-body, $K_6^{CC}(b)$ and $K_6^{BB}(b)$, and seven-body, $K_7^{BC}(a, b)$, solitary waves, because negative eigenvalues arise in the spectrum of the Hessian for these kinks.

To gain more precise knowledge about adiabatic motion we numerically solve the geodesic equation (1) for some different choices of the initial conditions $a(0)$, $b(0)$, $\dot{a}(0)$ and $\dot{b}(0)$. The values of the parameters $a(t)$ and $b(t)$ at $t = 0$ specify the initial static configuration $K_3^{OD}(a, b)$ and the soft perturbations on the kinks due to the zero modes $\frac{\partial \phi}{\partial a}$ and $\frac{\partial \phi}{\partial b}$ are determined by the values of the time-derivatives $\dot{a}(t)$ and $\dot{b}(t)$ at $t = 0$.

We first describe the scattering process when a perturbation due to the zero mode $\frac{\partial \phi}{\partial b}$ is exerted on a $K_3(0, b)$ kink with $|b|$ large. The initial solitary wave starts from some point in the green zone C of the moduli space (Figure 9) so that the configuration is formed by two lumps: a K_1^{OB} kink is on the right of the energy density profile and the superposition of a K_1^{BC} and a K_1^{CD} kink is on the left. These lumps approach each other, later crash into each other in the red zone A, and finally bounce back, recovering their original shape again in the other branch of green zone C, see Figure 17(a).

The process illustrated in Figure 17(b) is similar to the previous one. Here, a perturbation due to the zero mode $\frac{\partial \phi}{\partial a}$ is applied to a $K_3(a, 0)$ solitary wave. The initial configuration is formed by a K_1^{CD} lump and the superposition of a K_1^{BC} and a K_1^{OB} kink. The process of scattering is as follows: the two lumps approach each other in the green zone B, collide and travel superposed along the red zone A for

a period of time and finally split into two lumps, recovering the initial configuration in the other branch of green zone B.
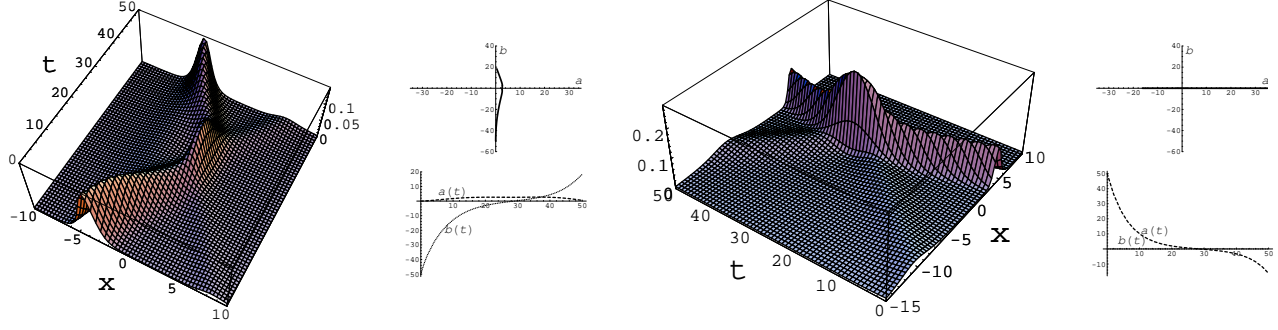

Figure 17: *Evolution of solitary waves.*

Although one of the two lumps is a composite of two basic particles, the phenomena described above are two-body scattering processes, essentially identical to the collisions of solitary waves studied in [20] and [14]. More sophisticated scattering processes are displayed in Figure 18, triggered by perturbations due to the two zero modes . *Genuine three-body low energy scattering arises, and as a result the main novelty in this paper emerges.*

First, start from a $K_3^{OD}(10, -70)$ solitary wave in the blue zone D near the border with the green zone C. In this configuration, the K_1^{CD} and K_1^{BC} kinks are close but the K_1^{OB} lump is far away from the other two, see Figure 18(a). A perturbation characterized by the values $\dot{b}(0) = -3$, $\dot{a}(0) = 6$ is exerted on this arrangement of lumps. The evolution of the solitary wave -unveiled from the corresponding geodesic found numerically- is as follows: the two closer particles collide and merge whereas the other particle goes towards them, all entering together in green zone C. The united lumps travel together and eventually split into the initial basic lumps -back again in a blue zone D of moduli space-, the K_1^{CD} moving towards the left and the K_1^{BC} towards the right on the line. Later, this lump bumps into the K_1^{OB} kink, which was traveling towards the left. The K_1^{BC} and the K_1^{OB} basic particles merge and move as a single one, -now in a green zone B-, and, after a certain time, they split, the whole solitary wave again entering in other blue zone D in the moduli space. Then, the K_1^{OB} kink advances towards the right and the K_1^{BC} advances towards the left on the line. Now this particle is attracted by the K_1^{CD} lump and they merge, coming again to a green zone C. In conclusion, the process can be interpreted as a interchange of the particle K_1^{BC} between the other particles K_1^{CD} and K_1^{OB}.

A last example of three-body collisions is displayed in Figure 18(b). A perturbation determined by $\dot{b}(0) = -3$, $\dot{a}(0) = 6$ is applied on a initial $K_3^{OD}(50, -50)$ solitary wave living in a blue zone D of the moduli space. The $K_3^{OD}(50, -50)$ configuration is formed by three separated basic particles. Note the apparent attractive forces between the lumps in Figure 18(b) showing the evolution of this solitary wave when the perturbation chosen above acts on it. The basic particles tend to approach each other at the beginning of the geodesic motion. More precisely, first the K_1^{OB} and K_1^{BC} lumps amalgamate when the geodesic enters a green zone B of the moduli space, then they travel together and, later on, they all merge together with the K_1^{CD} kink. During a period of time, when the geodesic passes through the red zone A, the three particles move together and, finally, a process of fission takes place in two stages. The K_1^{CD} kink splits from the global lump when the geodesic leaves the red zone to enter into the other green zone B, and later on so do the K_1^{OB} and K_1^{BC} kinks, the geodesic ending back in other blue zone D. This process may be repeated if the initial conditions setting the magnitude of the perturbation and the initial solitary wave are chosen adequately.
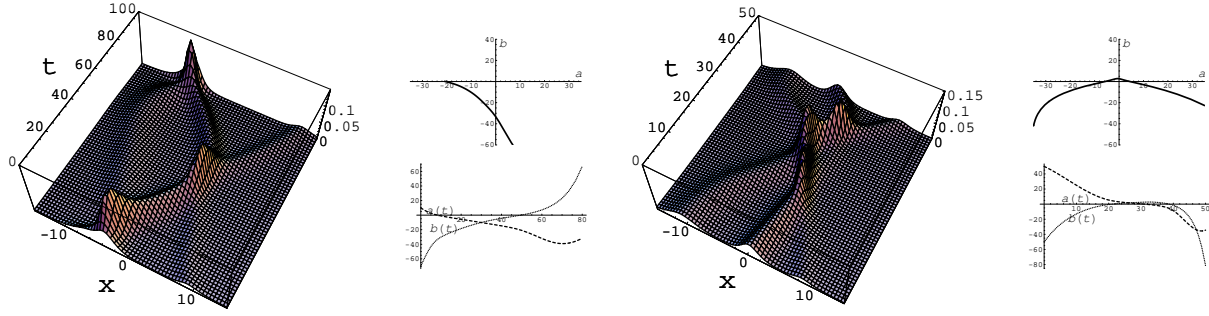
7

Figure 18: *Evolution of solitary waves.*

References

[1] P.G. Drazin, R.S. Johnson; *Solitons: an introduction.*, Cambridge University Press. 1989.

[2] A.H. Eschenfelder, *Magnetic Buble Technology*, (1981) Berlin, Springer-Verlag.

[3] F. Jona and G. Shirane, *Ferroelectric Crystals*, (1993) New York, Dover; E.K. Salje, *Phase Transitions in Ferroelastic and Co-Elastic Crystals*, Cambridge, UK, Cambridge University Press; B.A. Strukov and A. Levanyuk, *Ferroelectric Phenomena in Crystals*, Berlin, Springer-Verlag.

[4] F. Zhang and M. A. Collins *Topological solitons in polyethylene crystals*, Phys. Rev. E 49, 5804-5811 (1994); D. Bazeia and E. Ventura, *Topological twistons in crystalline polyethylene*, Chem. Phys. Lett., 303 (1999) 341-346; E. Ventura, A. M. Simas and D. Bazeia, *Exact topological twistons in crystalline polyethylene*, Chem. Phys. Lett., 320 (2000) 587-593; D. Bazeia, M.Z. Hernandes, A.M. Simas, *Solitons in Poly(oxyethylene)*, cond-mat/0207716.

[5] J.M. Harris, *Poly(ethylene glycol) chemistry: Biotechnical and Biomedical Applications*, (1992) New York, Plenum.

[6] A. Vilenkin and E.P.S. Shellard, *Cosmic Strings and Other Topological defects*, (1994) Cambridge, UK, Cambridge University Press.

[7] S. Kobayashi, K. Koyama and J. Soda, Phys. Rev. **D65** (2002) 064014; C. Csaki, J. Erlich, T.J. Hollowood and Y. Shirman, Nucl. Phys. **B581** (2000) 309-338; M. Cvetic, Int. J. Mod. Phys. **A16** (2001) 891-899; O. DeWolfe, D.Z. Freedman, S.S. Gubser, A.Karch, Phys. Rev. **D62** (2000) 046008

[8] H.M. Johng, H.S. Shin and K.S. Soh, Phys. Rev. **D53** (1996) 801; N.D. Antunes, E.J. Copeland, M. Hindmarsh and A. Lukas, *"Kinky brane worlds"*, Phys.Rev. D68 (2003) 066005

[9] T. Banks and M. O'Loughlin, Nucl. Phys. **B449**, (1995); T. Damour and A. Vilenkin, Phys. Rev. **D53** (1996) 2981; A. Wang, Phys. Rev **D66** (2002) 024024

[10] D. Olive and E. Witten, Phys. Lett. **B78** (1978) 97; N. Seiberg and E.Witten, Nucl. Phys. **B246** (1994) 19.

[11] M. Duff, R. Khuri and J. Lu, Phys. Rep. **259** (1995) 213.

[12] G. Dvali and M. Shifman, Nucl. Phys. **B504** (1997) 127; G. Gibbons and P. Townsend, Phys. Rev. Lett. **83** (1999) 172.

[13] R. Rajaraman, *Solitons and instantons. An introduction to solitons and instantons in quantum field theory*, North-Holland Publishing Co. 1987.

[14] A. Alonso Izquierdo, M.A. Gonzalez Leon, M. de la Torre Mayado, J. Mateos Guilarte, *"Changing shapes: adiabatic dynamics of composite solitary waves"*, Physica D **200** (2005) 220-241.

[15] C. Montonen, *"On solitons with an Abelian charge in scalar field theories: (I) Classical theory and Bohr-Sommerfeld quantization"*, Nucl. Phys. B **112** (1976) 349-357.

[16] H. Ito, *"Kink energy sum rule in a two-component scalar field model of 1+1 dimensions"*, Phys. Lett. A **112** (1985) 119-123.

[17] D. Bazeia, M. J. Dos Santos and R. F. Ribeiro, *"Solitons in systems of coupled scalar fields"*, Phys. Lett. A **208** (1995) 84-88.

[18] D. Bazeia, J. R. S. Nascimento, R. F. Ribeiro and D. Toledo, *"Soliton stability in systems of two real scalar fields"*, J. Phys. A **30** (1997) 8157-8166.

[19] A. Alonso Izquierdo, M.A. Gonzalez Leon, J. Mateos Guilarte and M. de la Torre Mayado, *"Kink variety in systems of two coupled scalar fields in two space-time dimensions"*, Phys. Rev. D **65** (2002) 085012.

[20] A. Alonso Izquierdo, M.A. Gonzalez Leon, J. Mateos Guilarte and M. de la Torre Mayado, *"Adiabatic motion of two-component BPS kinks"*, Phys. Rev. D **66** (2002) 105022.

[21] A. Alonso Izquierdo, M. A. Gonzalez Leon, and J. Mateos Guilarte, *"Kink manifolds in (1+1)-dimensional scalar field theory"*, J. Phys. A: Math. Gen. **31** (1998), 209-229.

[22] N. Manton, *"A remark on the scattering of BPS monopoles"*, Phys. Lett. B **110** (1982) 54-56.

[23] A. Alonso Izquierdo, M. A. Gonzalez Leon, and J. Mateos Guilarte, *"Kink from dynamical systems: domain walls in a deformed $O(N)$ linear sigma model"*, Nonlinearity **13** (2000), 1137-1169.

[24] A. Alonso Izquierdo, M. A. Gonzalez Leon, and J. Mateos Guilarte, *"Stability of kink defects in a deformed $O(3)$ linear sigma model"*, Nonlinearity **15** (2002), 1097-1125.

[25] A. Alonso Izquierdo, J.C. Bueno Sánchez, M. A. Gonzalez Leon, and M. de la Torre Mayado, *"Kink manifolds in a three-component scalar field theory"*, J. Phys. A: Math. Gen. **37** (2004), 3607-3626.

[26] D. Bazeia, L. Losano, C. Wotzasek, *"Domain walls in three-field models"*, Phys.Rev. **D66** (2002) 105025

[27] D. Bazeia and F. A. Brito, *Entrapment of a network of domain walls* Phys. Rev. **D62** (2000) 101701.

[28] P. Sutcliffe, *Domain wall networks on solitons*, Phys. Rev. **D68**, 085004 (2003).

[29] D. Bazeia, H. Boschi-Filho, F.A. Brito, *Domain defects in systems of two real scalar fields* JHEP **028** (1999) 9904; J.D. Edelstein, M.L. Trobo, F.A. Brito, D. Bazeia, *Kinks Inside Supersymmetric Domain Ribbons*, Phys.Rev. **D57** (1998) 7561-7569.

[30] J.R. Morris, *Nested Domain Defects* Int. J. Mod. Phys. **A13** (1998) 1115-1128.

[31] D. Bazeia, F.A. Brito, L. Losano, *Relaxing to a three dimensional brane junction*, hep-th/0512331.

[32] P.P. Avelino, C.J.A.P. Martins, J. Menezes, R. Menezes, J.C.R.E. Oliveira, *Defect Junctions and Domain Wall Dynamics*, hep-ph/0604250

[33] S. Coleman, *"There are no Goldstone bosons in two dimensions"*, Com. Math. Phys. **31** (1973) 259-264.

[34] H. Ito and H. Tasaki, *"Stability theory for nonlinear Klein-Gordon Kinks and Morse's index theorem"*, Phys. Lett. A **113** (1985) 179-182.

[35] J. Mateos Guilarte, *A note on Morse theory and one-dimensional solitons*, Lett. Math. Phys. **14** (1987) 169-176, *"Stationary phase approximation and quantum soliton families"*, Ann. Phys, **188** (1988) 307-346.